Schizophrenia Classification Using Resting State EEG Functional Connectivity: Source Level Outperforms Sensor Level

Sima Azizi[1], Daniel B. Hier[1], and Donald C. Wunsch II[1,2]

Abstract— Disrupted functional and structural connectivity measures have been used to distinguish schizophrenia patients from healthy controls. Classification methods based on functional connectivity derived from EEG signals are limited by the volume conduction problem. Recorded time series at scalp electrodes capture a mixture of common sources signals, resulting in spurious connections. We have transformed sensor level resting state EEG times series to source level EEG signals utilizing a source reconstruction method. Functional connectivity networks were calculated by computing phase lag values between brain regions at both the sensor and source level. Brain complex network analysis was used to extract features and the best features were selected by a feature selection method. A logistic regression classifier was used to distinguish schizophrenia patients from healthy controls at five different frequency bands. The best classifier performance was based on connectivity measures derived from the source space and the theta band.

Clinical relevance– The transformation of scalp EEG signals to source signals combined with functional connectivity analysis may provide superior features for machine learning applications.

I. INTRODUCTION

Schizophrenia (SZ) is a severe psychiatric disorder affecting approximately 1% of the US population [1]. There is compelling evidence that schizophrenics have abnormal structural and functional connectivity at both the microscopic and macroscopic scale [2]–[5]. Machine learning techniques have been used previously to distinguish schizophrenic patients from healthy controls based on brain connectivity [6]–[9].

Most studies of brain connectivity measurements in SZ patients have used fMRI data [6]–[8]; few have utilized abnormal EEG-based connectivity measures for classification [9], [10]. fMRI has less temporal resolution and higher costs than EEG. Most EEG-based classification studies have used scalp measurements. Due to the volume conduction problem, the recorded time series at scalp electrodes captures a mix of overlapping activities from common sensors. Brain connectivity measurements obtained at the scalp can suggest non-existent connections. We have compared classification using features derived from functional connectivity networks based on resting state EEG signals derived from both the sensor (scalp) space and the source (cortical) space.

[1] Department of Electrical & Computer Engineering, Missouri University of Science & Technology, Rolla, MO, USA (e-mail: sacc5,hierd,dwunsch@mst.edu)
[2] National Science Foundation, ECCS Division

II. METHODS

A. EEG Measurements

A previously published EEG data set of 14 schizophrenia patients (7 males: 27.9 ± 3.3 years, 7 females: 28.3 ± 4.1 years) and 14 control cases (7 males: 26.8 ± 2.9, 7 females: 28.7 ± 3.4 years) were utilized [11]. Each subject was recorded for fifteen minutes during a resting state eyes closed condition. The time series was recorded using a 10-20 standard system from 19 electrodes: Fp1, Fp2, F7, F3, Fz, F4, F8, T3, C3, Cz, C4, T4, T5, P3, Pz, P4, T6, O1, O2. The sampling frequency rate to acquire EEG signals was 250 Hz, with a reference electrode located at FCz. This research was exempt from Institutional Review Board approval based on the following exemption: projects limited to accessing and use of de-identified public datasets.

B. EEG preprocessing

Offline EEG preprocessing was done with MATLAB using Brainstorm [12]. The power line noise was removed using a notch filter at 50, 100 and 150 Hz. Data was high-passed with the cutoff frequency of 0.2 hz and low-passed with the cut off frequency of 50 hz to remove high-frequency noise including muscle artifacts. The reference electrode was changed offline according to the AVERAGE method. After visually inspecting the EEG signals and manually removing bad segments, signals were decomposed by independent component analysis (ICA) [13] using the Infomax algorithm in Brainstorm. Any non-cerebral independent components related to artifacts were removed manually and only components corresponding to cerebral activity were retained as a clean signal. A source reconstruction method was used to extract the source level EEG time series using Brainstorm [12]. This reconstruction depended on the exact spatial arrangement of the electrodes on the scalp (channel positions), an estimate of the geometrical and electrical properties of the head (head model), and the location and/or the orientation of the sources within the head (source model). The channel positions were imported into Brainstorm using the location of a 19 channel 10-20 standard EEG system. The head model was obtained by the boundary element method in OPEN-MEEG based on the default anatomy in the Brainstorm (ICBM152 anatomy). The source model was created by randomly distributing 15000 sources at the cortex with the orientation of the sources perpendicular to the surface. The time series of the sources were computed using the minimum norm estimate (MNE) method with an identity matrix as the noise covariance. EEG signals at source and sensor levels

were filtered into frequency bands of 2-4 Hz (delta), 4-7 Hz (theta), 8-13 Hz (alpha), 13-30 Hz (beta), and 30-45 Hz (gamma).

C. Functional Connectivity Computations

Source and sensor level EEG time series were divided into epochs as quasi-stationary time series, each with a duration of 2 minutes. Functional connectivity measures were computed for the first 2 minute epoch by computing the phase lag index (PLI) [14] between any two brain regions. Phase lag index (PLI) is less sensitive to the volume conduction problem and is bounded between 0 and 1. PLI is zero if there is no coupling or coupling is around phase 0 mode π. PLI is 1 if there is phase locking or the phase difference is other than 0 mode π. The brain networks are considered as a graph of N nodes (each representing different brain regions) with E edges (each representing the connection between pairs of nodes).

D. Graph Metric Computation

The brain network metrics were computed using complex network analysis from MATLAB [15]. Eleven graph metrics were selected for analysis: strength, transitivity, betweenness centrality, participation coefficient, local efficiency, ratio of local to global efficiency (RL2GE), modularity, assortativity, characteristic path, and small worldness. A brief explanation of each metric follows [15].

The simplest graph metric is *degree*, defined as the number of edges connected to a node. *Strength*, a weighted variation of degree, is the sum of all the neighboring link weights for each node. *Betweenness centrality* is the fraction of all shortest paths passing through a specific node. Clustering coefficient is the tendency of the nodes in a network to create clusters. It is calculated as the fraction of triangles (three fully connected nodes) to the triplets (three nodes that are not fully connected) in the network. *Transitivity* is a variation of the clustering coefficient utilizing a different normalization method. *Modularity* specifies the degree to which a network can be divided into non overlapping subgroups of nodes, such that the number of within-group edges is maximized and the number of between-group edges is minimized. *Characteristic path* is defined as the average shortest path length in a network and *global efficiency* measures the average inverse shortest path length in the network (characteristic path reflects longer paths and global efficiency reflects shorter paths). We also calculated the ratio of local efficiency to global efficiency. *Assortativity* is the correlation coefficient between the degrees of all nodes on two opposite ends of a link. A positive assortativity coefficient reflects a network with a strong core of mutually interconnected high-degree hubs. In contrast, a negative assortativity coefficient reflects a network with widely distributed high-degree hubs. Small-world networks are a middle ground between regular and random networks, while containing high transitivity (like regular networks), yet exhibiting small characteristic path length (like random networks). To quantify *small worldnesss*, the ratio of transitivity to characteristic path length of the

graph was calculated and compared to the same quantity computed for its equivalent random graph. *Participation coefficient* is the extent to which scattered nodes connect to other modules. High participation coefficients indicate a node which is connected uniformly across all modules, while a low participation coefficient reflects a node which is more connected to the nodes within its own module.

E. Feature Selection and Classification

We examined multiple feature selection methods to reduce the number of input features and improve classifier performance. We selected a univariate filter algorithm to rank features by the ANOVA F-score. Based on empirical performance, we selected k=10 features to enter into a logistic regression classifier. A 10-fold cross validation strategy was used to evaluate model performance including accuracy, sensitivity and specificity (mean $\pm$ SD).

III. RESULTS

The location and amplitude of the reconstructed sources are displayed in a 3D graph at 2 nominal time values in Fig. 1. High amplitude brain activity is observed over the right temporal lobe at the 70 second time-point and over both occipital areas at the 120 second time-point. The time series generated by the source electrodes were projected onto 148 ROIs as defined by the Destrieux Atlas [16]. Mapping was done by flipping the orientation of sources in the opposite direction and averaging them over an ROI.

Functional connectivity networks were computed for each subject in the source and sensor spaces. Connectivity measures were computed over 2 minute epochs for each subject. The network was represented as a $N*N$ weighted adjacency matrix where rows and columns corresponded to a specific brain region and each cell corresponded to the connectivity measure between the column region and the row region. For the sensor space, N is the number of EEG channels ($N = 19$) and for the source space N is the number of region of interest ($N = 148$). The diagonal (identity) elements were set to zero. The adjacency matrices were obtained for five distinct frequency bands. Thresholds were set for values in the weighted adjacency matrices to preserve a p portion of
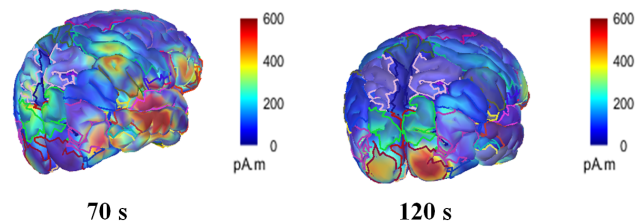

70 s   **120 s**

Fig. 1. Source reconstruction. Source level brain signals are estimated using the minimum norm estimate (MNE) method in Brainstorm software. The head model is obtained using the boundary element method in OPEN-MEEG based on the default anatomy in the Brainstorm (ICBM152 anatomy) and the source model is created by randomly distributing 15000 sources at the cortex surface with perpendicular orientation to the surface. Color scale reflects amplitude of source level signals prior to connectivity analysis.
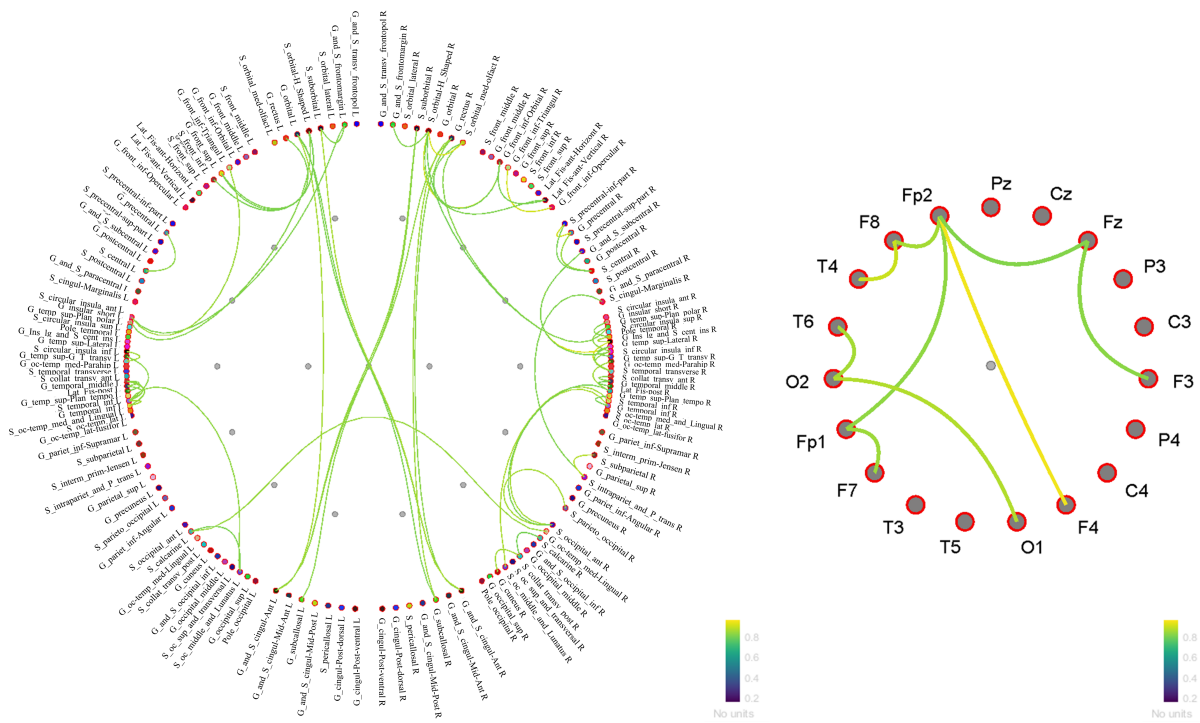
Fig. 2. Functional connectivity graph for the alpha band displayed for one subject. The graphs demonstrate 20% of the strongest connections in the network. For the source-based graph, the nodes are arranged right-left symmetrically. For the sensor-based graph, the arrangement of electrodes is not right-left symmetric. Left-sided electrodes are odd numbered, right-sided electrodes are even numbered (e.g. F4, T4, T6) by convention. **Left**: Functional connectivity graph for the source space. **Right**: Functional connectivity graph for the sensor space.

TABLE I

GROUP MEANS AND ANOVA F-VALUES FOR THE TEN HIGHEST-RANKING FEATURES FROM THE SOURCE AND SENSOR SPACES (THETA BAND)

Graph metric	Source Space ROIs	SZ mean	Control mean	ANOVA F-value
Strength	Inferior temporal sulcus L	29.01	36.39	29.60
Ratio of local to global efficiency	Transverse temporal sulcus L	1.32	1.29	17.47
Ratio of local to global efficiency	Posterior ramus of the lateral sulcus L	1.24	1.20	14.64
Ratio of local to global efficiency	Temporal pole L	1.22	1.20	13.03
Ratio of local to global efficiency	Planum temporale L	1.28	1.26	12.47
Ratio of local to global efficiency	Anterior transverse temporal gyrus L	1.22	1.17	11.39
Strength	Calcarine sulcus R	34.83	30.77	35.43
Strength	Inferior temporal sulcus R	27.89	36.11	10.85
Strength	Inferior part of the precentral sulcus R	16.51	21.09	10.66
Ratio of local to global efficiency	Parahippocampal gyrus L	1.21	1.23	10.39
Graph metric	Sensor Space ROIs	SZ Mean	Control Mean	ANOVA F-value
Betweeness centrality	O2	22.61	42.28	32.38
Participation coefficient	Cz	0.31	0.39	9.93
Participation coefficient	T5	0.11	0.27	6.20
Betweeness centrality	F7	16.76	21.14	5.98
Participation coefficient	O2	0.51	0.57	5.72
Clustering Coefficient	P3	0.34	0.29	5.62
Transitivity	Global measure	0.42	0.38	5.23
Strength	F7	3.2	3.70	4.81
Participation coefficient	C4	0.21	0.23	4.75
Local Efficiency	Fp2	0.56	0.54	4.49

TABLE II

COMPARISON OF THE SCHIZOPHRENIA CLASSIFIER IN BOTH SOURCE AND SENSOR SPACE USING EEG-BASED FUNCTIONAL CONNECTIVITY AT DIFFERENT FREQUENCY BANDS

Source Space	Alpha	Theta	Beta	Delta	Gamma
Accuracy	0.93 ($\pm$0.18)	0.97 ($\pm$0.13)	0.93 ($\pm$0.18)	0.75 ($\pm$0.19)	0.92 ($\pm$0.20)
Sensitivity	0.93 ($\pm$0.27)	0.95 ($\pm$0.25)	0.90 ($\pm$0.30)	0.67 ($\pm$0.38)	0.93 ($\pm$0.27)
Specificity	0.91 ($\pm$0.22)	0.98 ($\pm$0.23)	0.92 ($\pm$0.28)	0.80 ($\pm$0.32)	0.90 ($\pm$0.23)
Sensor Space	Alpha	Theta	Beta	Delta	Gamma
Accuracy	0.71 ($\pm$0.26)	0.89 ($\pm$0.30)	0.86 ($\pm$0.28)	0.70 ($\pm$0.57)	0.73 ($\pm$0.40)
Sensitivity	0.67 ($\pm$0.30)	0.90 ($\pm$0.23)	0.67 ($\pm$0.30)	0.67 ($\pm$0.32)	0.60 ($\pm$0.45)
Specificity	0.70 ($\pm$0.23)	0.93 ($\pm$0.27)	0.70 ($\pm$0.43)	0.73 ($\pm$0.27)	0.60 ($\pm$0.32)

the strongest weights for each brain network. To select the optimal value for p, a search was conducted over the interval $[0.01, 0.8]$ with incremental steps of 0.01. The value of 0.19 yielded the best classifier performance. Each subject was represented as a graph. Functional connectivity graphs at the source and sensor space in the alpha band are shown for one subject (Fig. 2).

Brain complex network analysis was employed to create a feature vector for each subject. For each local measure, N (the number of nodes in the network) features were calculated. The five local measures (strength, betweenness centrality, participation coefficient, local efficiency and ratio of local to global efficiency) generate 5*N features and are added to five global features (modularity, transitivity, assortativity, characteristic path length and small worldness), giving $5 * 148 + 5 = 745$ features in the source space and $5 * 19 + 5 = 100$ features in the sensor space.

Based on a univariate feature filter, we selected the 10 best features from the source and sensor spaces to enter into a logistic regression classifier. Table I shows the region of interest and the graph metric for the ten highest ranking features that differentiated between the SZ and control groups (ANOVA F-values). For instance, inferior temporal sulcus at the left side of the head has higher *strength* in the control groups compared to SZ patients. Similarly, *betweenness centrality* at O2 electrode is higher for controls compared to SZ patients. The classification model derived from functional connectivity measures from the source space outperformed the model based on the sensor space (Table II. Classification performance differed by frequency band with the best classification performance was observed for the theta band in the source space. This supports the findings of [17], who found a higher functional connectivity for most of the ROI pairs for SZ patients as compared to healthy subjects. Also, [18] found increased brain connectivity in the theta band for schizophrenia subjects.

IV. CONCLUSIONS

We discriminated between schizophrenia patients and healthy controls using functional connectivity measurements derived from resting state EEG recordings. The sensor level EEG recordings at the scalp were transformed to source space EEG time series by source reconstruction. The phase lag index was used to calculate the functional connectivity network. Complex brain network analysis was used to characterize the quantitative features of each network. A logistic regression classifier was used to distinguish SZ patients from healthy controls based on a subset of the most significant features. The performance of the classifier was compared for the sensor space and source space at five different frequency bands: alpha, theta, beta, delta and gamma. Better classifier performance was observed using the source space and the theta band. Previously, quantitative EEG (qEEG) has been used for classification, using the power at various locations and frequencies [19]. Connectivity analysis provides an alternative approach to the derivation

of features for classifiers. In the future, we plan head-to-head comparisons of classifiers using qEEG derived features against connectivity-derived features.

REFERENCES

[1] R. J. Wyatt, I. Henter, M. C. Leary, and E. Taylor, "An economic evaluation of schizophrenia-1991," *Social psychiatry and psychiatric epidemiology*, vol. 30, no. 5, pp. 196–205, 1995.

[2] M.-E. Lynall, D. S. Bassett, R. Kerwin, P. J. McKenna, M. Kitzbichler, U. Muller, and E. Bullmore, "Functional connectivity and brain networks in schizophrenia," *Journal of Neuroscience*, vol. 30, no. 28, pp. 9477–9487, 2010.

[3] V. D. Calhoun, J. Sui, K. Kiehl, J. A. Turner, E. A. Allen, and G. Pearlson, "Exploring the psychosis functional connectome: aberrant intrinsic networks in schizophrenia and bipolar disorder," *Frontiers in psychiatry*, vol. 2, p. 75, 2012.

[4] K. J. Friston and C. D. Frith, "Schizophrenia: a disconnection syndrome," *Clin Neurosci*, vol. 3, no. 2, pp. 89–97, 1995.

[5] M. P. Van Den Heuvel and A. Fornito, "Brain networks in schizophrenia," *Neuropsychology review*, vol. 24, no. 1, pp. 32–48, 2014.

[6] M. R. Arbabshirani, K. Kiehl, G. Pearlson, and V. D. Calhoun, "Classification of schizophrenia patients based on resting-state functional network connectivity," *Frontiers in neuroscience*, vol. 7, p. 133, 2013.

[7] H. Shen, L. Wang, Y. Liu, and D. Hu, "Discriminative analysis of resting-state functional connectivity patterns of schizophrenia using low dimensional embedding of fmri," *Neuroimage*, vol. 49, no. 4, pp. 3110–3121, 2010.

[8] J. I. Arribas, V. D. Calhoun, and T. Adali, "Automatic bayesian classification of healthy controls, bipolar disorder, and schizophrenia using intrinsic connectivity maps from fmri data," *IEEE Transactions on Biomedical Engineering*, vol. 57, no. 12, pp. 2850–2860, 2010.

[9] C.-R. Phang, C.-M. Ting, S. B. Samdin, and H. Ombao, "Classification of eeg-based effective brain connectivity in schizophrenia using deep neural networks," in *2019 9th International IEEE/EMBS Conference on Neural Engineering (NER).* IEEE, 2019, pp. 401–406.

[10] Q. Chang, M. Liu, Q. Tian, H. Wang, Y. Luo, J. Zhang, and C. Wang, "Eeg-based brain functional connectivity in first-episode schizophrenia patients, ultra-high-risk individuals, and healthy controls during p50 suppression," *Frontiers in human neuroscience*, vol. 13, p. 379, 2019.

[11] E. Olejarczyk and W. Jernajczyk, "Graph-based analysis of brain connectivity in schizophrenia," *PLoS One*, vol. 12, no. 11, p. e0188629, 2017.

[12] F. Tadel, S. Baillet, J. Mosher, D. Pantazis, and R. Leahy, "Brainstorm: a user-friendly application for meg/eeg analysis computational intelligence and neuroscience," *Hindawi Publishing Corporation*, pp. 1–13, 2011.

[13] S. Makeig, A. J. Bell, T.-P. Jung, T. J. Sejnowski *et al.*, "Independent component analysis of electroencephalographic data," *Advances in neural information processing systems*, pp. 145–151, 1996.

[14] C. J. Stam, G. Nolte, and A. Daffertshofer, "Phase lag index: assessment of functional connectivity from multi channel eeg and meg with diminished bias from common sources," *Human brain mapping*, vol. 28, no. 11, pp. 1178–1193, 2007.

[15] M. Rubinov and O. Sporns, "Complex network measures of brain connectivity: uses and interpretations," *Neuroimage*, vol. 52, no. 3, pp. 1059–1069, 2010.

[16] C. Destrieux, B. Fischl, A. Dale, and E. Halgren, "Automatic parcellation of human cortical gyri and sulci using standard anatomical nomenclature," *Neuroimage*, vol. 53, no. 1, pp. 1–15, 2010.

[17] G. Di Lorenzo, E. Daverio, F. Ferrentino, E. Santarnecchi, F. Ciabattini, L. Monaco, G. Lisi, Y. Barone, C. Di Lorenzo, C. Niolu *et al.*, "Altered resting-state eeg source functional connectivity in schizophrenia: the effect of illness duration," *Frontiers in human neuroscience*, vol. 9, p. 234, 2015.

[18] C. Andreou, G. Leicht, G. Nolte, N. Polomac, S. Moritz, A. Karow, I. L. Hanganu-Opatz, A. K. Engel, and C. Mulert, "Resting-state theta-band connectivity and verbal memory in schizophrenia and in the high-risk state," *Schizophrenia research*, vol. 161, no. 2-3, pp. 299–307, 2015.

[19] T. Xu, M. Stephane, and K. K. Parhi, "Abnormal neural oscillations in schizophrenia assessed by spectral power ratio of meg during word processing," *IEEE Transactions on Neural Systems and Rehabilitation Engineering*, vol. 24, no. 11, pp. 1148–1158, 2016.